Reciprocal electromechanical properties of rat prestin: The motor molecule from rat outer hair cells

Jost Ludwig*†, Dominik Oliver*†, Gerhard Frank‡, Nikolaj Klöcker*, Anthony W. Gummer‡, and Bernd Fakler*§

*Department of Physiology II, Ob dem Himmelreich 7, 72074 Tübingen, Germany; and ‡Department of Otolaryngology, Section of Physiological Acoustics and Communication, Silcherstr. 5, 72076 Tübingen, Germany

Edited by A. James Hudspeth, The Rockefeller University, New York, NY, and approved February 2, 2001 (received for review December 23, 2000)

Cochlear outer hair cells (OHCs) are responsible for the exquisite sensitivity, dynamic range, and frequency-resolving capacity of the mammalian hearing organ. These unique cells respond to an electrical stimulus with a cycle-by-cycle change in cell length that is mediated by molecular motors in the cells' basolateral membrane. Recent work identified prestin, a protein with similarity to pendrin-related anion transporters, as the OHC motor molecule. Here we show that heterologously expressed prestin from rat OHCs (rprestin) exhibits reciprocal electromechanical properties as known for the OHC motor protein. Upon electrical stimulation in the microchamber configuration, rprestin generates mechanical force with constant amplitude and phase up to a stimulus frequency of at least 20 kHz. Mechanical stimulation of rprestin in excised outside-out patches shifts the voltage dependence of the nonlinear capacitance characterizing the electrical properties of the molecule. The results indicate that rprestin is a molecular motor that displays reciprocal electromechanical properties over the entire frequency range relevant for mammalian hearing.

Outer hair cells (OHCs) of the mammalian cochlea exhibit the unique property of actively changing their cell length in response to changes in the membrane potential (1–3): the cell shortens upon depolarization and lengthens when hyperpolarized. This electromotility occurs at acoustic frequencies (4, 5) and is believed to provide a basis for the cochlear amplifier, a local mechanical amplification mechanism within the organ of Corti (6), that enables the high sensitivity, dynamic range, and frequency selectivity of hearing in mammals.

The mechanism underlying electromotility has been tracked down to an intrinsic property of the OHC basolateral membrane: (*i*) OHC motility is directly driven by the transmembrane voltage and is independent of Ca^{2+} influx or ATP supply (7, 8); (*ii*) it works in a cycle-per-cycle mode at frequencies up to at least 70 kHz, faster than any other biological force generator including myosin or kinesin (4, 5, 9); (*iii*) it is accompanied by a charge movement (or gating current) that can be measured as a nonlinear capacitance (C_{nonlin}) and shares voltage dependence and a panel of antagonists with the motility itself (10–12); and (*iv*) changes in mechanical membrane tension cause a shift of C_{nonlin} along the voltage axis (13–15).

These findings have led to the hypothesis of an integral membrane protein, termed the motor protein, as the molecular element underlying fast OHC motility (7, 16). In response to changes in the transmembrane voltage, the motor protein is thought to undergo a structural rearrangement that changes its area in the plasma membrane (17, 18). As a result of the concerted action of a large number of motor molecules supposed to be densely packed in the OHC basolateral membrane (19), the cell changes its length by up to 5%. In this concept, the voltage dependence of electromotility is brought about by a charged voltage sensor within the motor protein that translocates upon changes in membrane potential and thus initiates the conformational change generating mechanical energy. In turn, a change in mechanical energy will act back onto the movement of the protein's voltage sensor, which will result in a shift of C_{nonlin} on the voltage axis (18). Therefore, the motor protein is thought to exhibit quasi-piezoelectrical properties: it generates mechanical force upon electrical stimulation and changes its electrical properties upon mechanical stimulation.

Using a differential cloning strategy, Dallos and coworkers (20) recently have identified the cDNA of a so-far unknown protein from gerbil called prestin, that is specifically expressed in OHCs and shows homology with the family of pendrin-related anion transporters. When expressed in a mammalian cell line, prestin showed hallmarks of the OHC motor protein, including voltage-dependent C_{nonlin} and cell motility upon electrical stimulation.

The landmark cloning of prestin now allows testing of the concept of a single protein working as a bidirectional converter of electrical and mechanical energy in the absence of the highly specialized membrane-associated structures of the OHC (21) or of the specific lipid composition of its membrane.

Here we investigate reciprocal electromechanical properties of the rat homologue of prestin (rprestin) by using force measurements in the microchamber configuration with stimulus frequencies in the tens of kHz range and recording of C_{nonlin} in excised patches under variation of the membrane tension.

Materials and Methods

Molecular Biology. Several oligonucleotide primers were deduced from a murine bacterial artificial chromosome clone (derived from chromosome 5; GenBank accession no. AC083284) that comprises most of the mouse prestin gene and was retrieved by a database search using the gerbil prestin sequence (20). When used in PCR experiments with rat cochlea-cDNA as template, these primers amplified a short fragment of the rprestin cDNA (nucleotides 70–470; numbers referring to the rprestin coding region). Using this sequence stretch as an anchor, 5′ and 3′ rapid amplification of cDNA ends protocols were applied to isolate further rprestin fragments from a rat cochlea cDNA library (22, 23). Together, the fragments covered a total of 3,041 nt, including the complete coding sequence of rprestin (GenBank accession no. AJ303372).

Overlapping 5′ and 3′ fragments of the rprestin coding sequence were combined by using a PCR-based overlap extension (24); recognition sequences for *Bam*HI and *Hin*dIII were

This paper was submitted directly (Track II) to the PNAS office.

Abbreviations: OHC, outer hair cell; C_{nonlin}, nonlinear capacitance; rprestin, rat homologue of prestin; CMV, cytomegalovirus; GFP, green fluorescent protein; OK, opossum kidney; CHO, Chinese hamster ovary; HEK, human embryonic kidney; C_{m}, membrane capacitance; AFL, atomic force lever.

Data deposition: The sequence reported in this paper has been deposited in the GenBank database (accession no. AJ303372).

†J.L. and D.O. contributed equally to this work.

§To whom reprint requests should be addressed. E-mail: bernd.fakler@uni-tuebingen.de.

The publication costs of this article were defrayed in part by page charge payment. This article must therefore be hereby marked "*advertisement*" in accordance with 18 U.S.C. §1734 solely to indicate this fact.

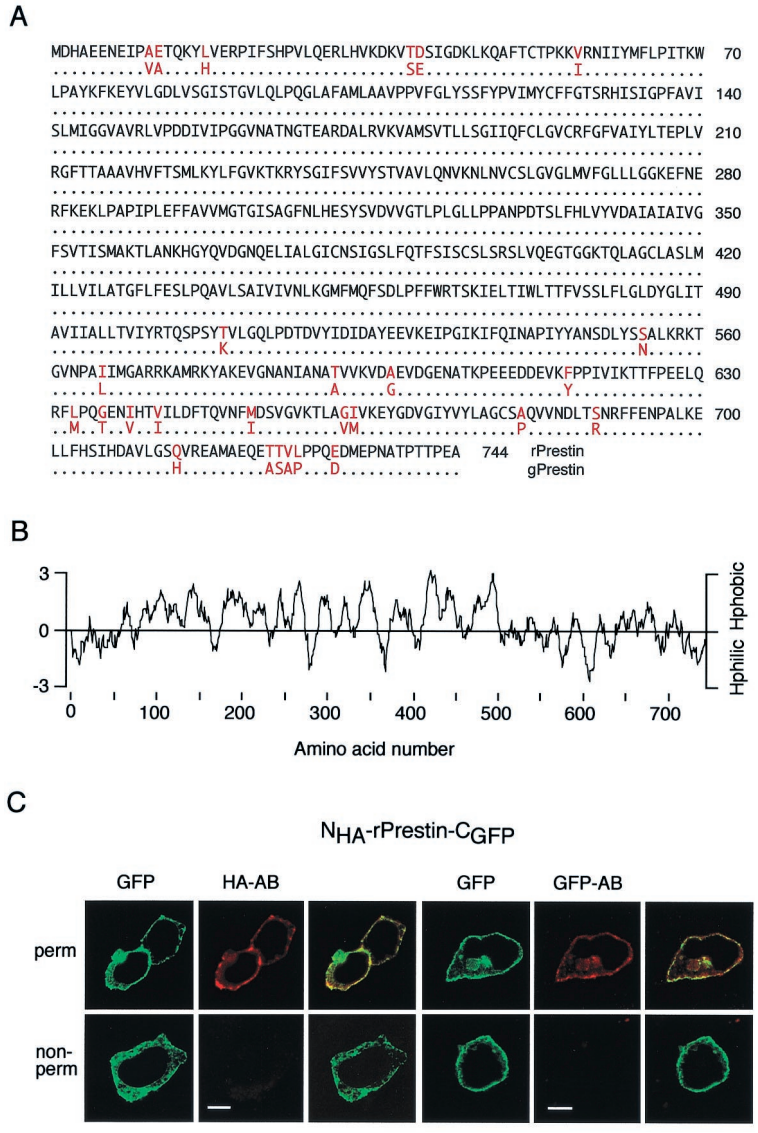

Fig. 1. Amino acid sequence of rprestin and localization of its N and C termini to the cytoplasmic side. (*A*) Sequence comparison between the prestin molecules from rat and gerbil (gprestin); identical residues are indicated by dots, residues different between both sequences are given in red. (*B*) Hydropathy plot for rprestin calculated from the algorithm by Kyte and Doolittle with an amino acid window of 12 residues. Hphobic, hydrophobic; Hphilic, hydrophilic. (*C*) Antibodies to HA (HA-AB) and GFP (GFP-AB) bind to their targets fused to the N terminus (HA) and C terminus (GFP) of rprestin (N_{HA}-rprestin-C_{GFP}) only if OK cells were permeabilized (*Upper*); no binding is observed in nonpermeabilized cells (*Lower*). Images for either experiment are GFP fluorescence, cy-3 fluorescence indicating staining of HA-AB or GFP-AB, and overlay of both. (Scale bars are 10 μm.)

introduced at the 5′ and 3′ ends for subcloning and nucleotides −5 to −1 were changed to match the Kozak consensus-sequence for translation initiation (25, 26). The final PCR product was ligated into the eukaryotic expression plasmid vector pBK-CMV (cytomegalovirus) (Stratagene), yielding pBK-CMV-rprestin. GLUT5 cDNA was subcloned into pBK-CMV by using restriction digest to yield pBK-CMV-GLUT5.

N- and C-terminal fusion constructs were made as follows: (*i*) the N-terminal hemagglutinin (HA)-tagged rprestin expression construct (pBK-CMV-N_{HA}-rprestin) was obtained by ligating a double-stranded oligonucleotide encoding the HA tag (*AYPYDVPDY*) carrying *Spe*I and *Bam*HI-compatible protruding ends into *Spe*I/*Bam*HI-digested pBK-CMV-rprestin; (*ii*) the green fluorescent protein (GFP)-mut3 coding sequence was fused to the 3′ end of rprestin by using PCR-based overlap extension. The PCR product was reinserted into pBK-CMV-rprestin and pBK-CMV-N_{HA}-rprestin by using *Bst*1107I (nucleotide 1557 in the rprestin sequence) and *Hin*dIII sites, yielding pBK-CMV-rprestin-C_{GFP} and pBK-CMV-N_{HA}-rprestin-C_{GFP}, respectively.

Immunocytochemistry. Opossum kidney (OK) cells (American Type Culture Collection) were grown and transfected as described (27). For immunocytochemistry, cells were fixed in 4% paraformaldehyde in PBS for 15 min at 4°C and blocked with 10% normal goat serum (NGS) in PBS containing 0.05% Triton X-100 (PBS-T) for 1 h at room temperature. Subsequently, cells were incubated with the following primary antibodies: mouse monoclonal anti-GFP (CLONTECH), mouse monoclonal anti-HA (Santa Cruz Biotechnology), and rabbit polyclonal anti-GLUT5 (Chemicon), each diluted at 1:200 in 2% NGS/PBS-T.

Immunoreactivity was revealed by cy-3-conjugated anti-mouse antiserum. For investigating the topology of the N and C termini of rprestin, experiments were repeated without mem-

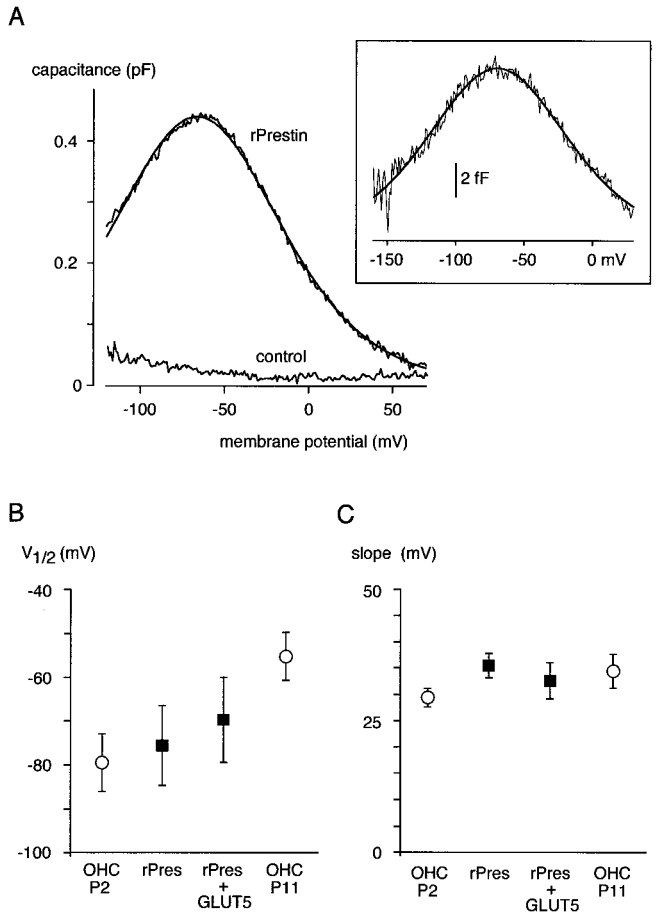

Fig. 2. Gating charge movement measured as C_{nonlin} in CHO cells expressing rprestin. (*A*) C_{nonlin} measured with the phase-tracking technique in response to a voltage ramp from −120 to 70 mV. Line is fit of Eq. **1** to data with values for the fit parameters of −66.3 mV ($V_{1/2}$), 33.3 mV (α), and 58.6 fC (Q_{max}). (*Inset*) C_{nonlin} measured in an excised outside-out patch in response to a voltage ramp from −160 to 30 mV; data are average of four ramp recordings, fit parameters were −69.5 mV ($V_{1/2}$), 34.3 mV (α), and 1.4 fC (Q_{max}). (*B* and *C*) Values of $V_{1/2}$ and slope obtained for C_{nonlin} in experiments as in *A* from CHO cells expressing rprestin either alone or together with GLUT5 (expression verified by a GLUT5-specific antibody); data are mean ± SD of 16 and 7 experiments, respectively. $V_{1/2}$ and slope values obtained from rat OHCs of postnatal stages P2 and P11 are included for comparison.

brane permeabilization. To this end, either living cells were incubated with the primary antibody (diluted at 1:200 in medium) for 40 min at 4°C and fixed only before secondary antibody incubation or fixed cells were stained following the above protocol, omitting Triton X-100. Samples were imaged with a confocal laser scanning microscope (LSM 510, Zeiss).

Electrophysiology. For electrophysiological experiments, the expression plasmids pBK-CMV-rprestin, pBK-CMV-rprestin-C_{GFP}, and pBK-CMV-GLUT5 (GenBank accession no. D28562) were injected into Chinese hamster ovary (CHO) cells by using a microinjector (Transjector 5246, Eppendorf), or were transfected to CHO cells, OK cells, or human embryonic kidney (HEK) 293 cells with the effectene transfection reagent (Qiagen, Hilden, Germany). Recordings from OHCs were performed by using acutely isolated organs of Corti from rats, as described (28). Whole-cell patch-clamp recordings were done with an Axopatch 200B amplifier (Axon Instruments, Foster City, CA) at room temperature (21–24°C). Electrodes were pulled from quartz glass, had resistances of 2–3 MΩ, and were coated with Sylgard. Whole-cell series resistances ranged from 2.4 to 8 MΩ. For recordings on culture cells and for outside-out patch experiments, electrodes were filled with a solution containing: 135 mM KCl, 3.5 mM $MgCl_2$, 0.1 mM $CaCl_2$, 5 mM K_2EGTA, 5 mM Hepes, mM 2.5 Na_2ATP. For OHC whole-cell recordings, the composition of the pipette solution was: 125 mM KCl, 20 mM tetraethylammonium-chloride, 3.5 mM $MgCl_2$, 0.1 mM $CaCl_2$, 5 mM K_2EGTA, 2.5 mM Na_2ATP, 5 mM Hepes, pH adjusted to 7.3 with KOH. During recordings the bath was continuously perfused with a solution containing: 144 mM NaCl, 5.8 mM KCl, 1.3 mM $CaCl_2$, 0.9 mM $MgCl_2$, 10 mM Hepes, 0.7 mM Na_2HPO_4, 5.6 mM glucose, adjusted to pH 7.3 with NaOH. Osmolarity of all solutions was adjusted to 305 ± 2 mOsm with glucose. Outside-out patches were excised from transfected cells or from the lateral membrane of OHCs after a quick test for C_{nonlin} in the whole-cell mode. Pressure of variable amplitude was generated with the Eppendorf microinjector (regulated output) and applied to the recording pipette via a hand-switched valve; the pressure output displayed by the microinjector was monitored and used in pressure-capacitance relations (see Fig. 4*C*).

Voltage-dependent capacitance was measured by using a software-based lock-in technique (phase tracking) as described (29, 30). Briefly, after manual compensation of membrane capacitance (C_m), lock-in phase angles, yielding signals proportional to changes in C_m and conductance, were calculated by dithering the series resistance by 0.5 MΩ. The capacitance output was calibrated by a 100-fF change of the C_m compensation setting. Command sinusoid (f = 1–5 kHz, usually 2.6 kHz; 10 mV) was filtered at 2.5 f with an 8-pole Bessel filter, and 16 periods were averaged to generate each capacitance point. To obtain the voltage dependence of C_m, voltage ramps ranging from −120 to + 70mV or −160 to +30 mV (slope 0.16 Vs^{-1}) were summed to the sinusoid command during capacitance measurements. Scaled capacitance traces induced by the voltage ramp were plotted versus membrane voltage. Capacitance was fitted with the derivative of a Boltzmann function (11),

$$C(V) = C_{lin} + \frac{Q_{max}}{\alpha e^{\frac{V - V_{1/2}}{\alpha}} \left(1 + e^{-\frac{V - V_{1/2}}{\alpha}}\right)^2}, \qquad [1]$$

where C_{lin} is residual linear membrane capacitance, not compensated for by the C_m compensation circuit of the amplifier, V is membrane potential, Q_{max} is maximum voltage sensor charge moved through the membrane electrical field, $V_{1/2}$ is voltage at half-maximum charge transfer, and α is the slope factor of the voltage dependence.

Processing and fitting of data were performed with IGORPRO (WaveMetrics, Lake Oswego, OR) on a Macintosh PowerPC; all data are given as mean ± SD.

Force Measurements. Electromechanical forces generated by rprestin in transfected cells (HEK 293, CHO) were measured as described (5). Briefly, solitary cells were sucked into a heat-polished glass capillary, termed the microchamber (31), with an opening diameter between 10 and 13 μm. Transfected cells could be easily distinguished from nontransfected cells because of the strong fluorescence of rprestin-C_{GFP} (see Fig. 3). The glass capillary and the bath chamber were filled with Hanks' balanced salt solution (Sigma, supplemented with $NaHCO_3$ and 10 mM Hepes), adjusted to 300 mOsm and pH 7.4. Force was derived from the velocity of an atomic force lever (AFL; Nanosensors, Wetzlar-Blankenfeld, Germany), the reverse side of which was gently placed against the exposed surface of the cell (see Fig. 3); the contact area was 170–300 μm^2. All AFLs had spring constants around 0.03 N/m and were calibrated before the first

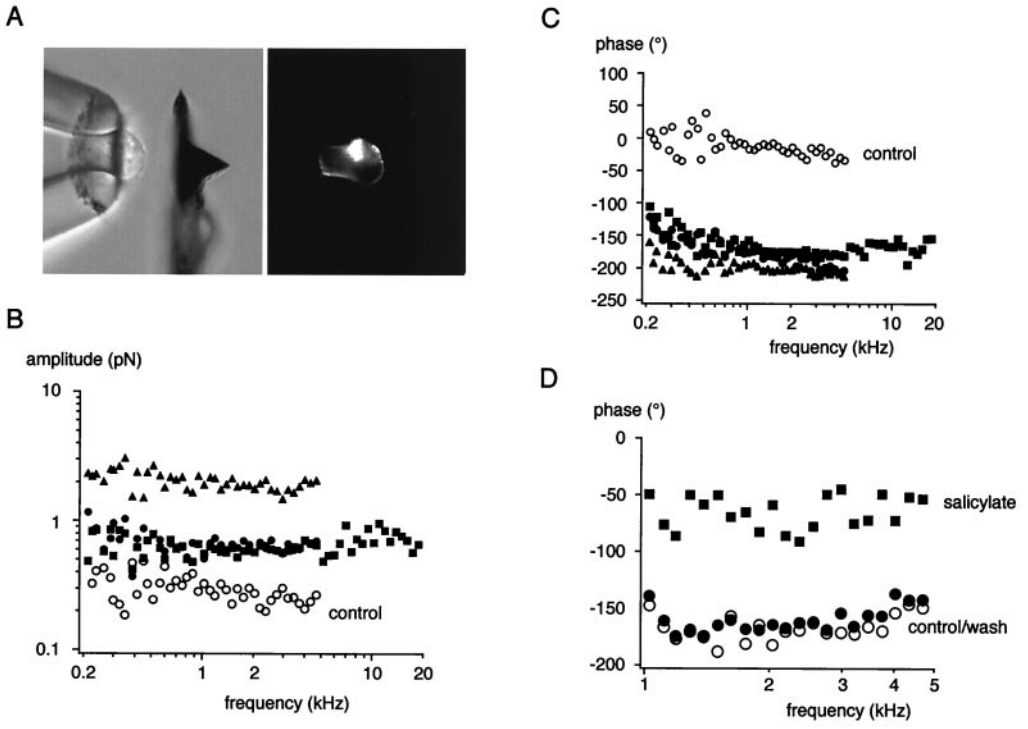

Fig. 3. Mechanical force generated by rprestin in response to electrical stimulation. (*A*) Experimental configuration with a transfected HEK293 cell sucked roughly halfway into the microchamber and the AFL placed close to it (*Left*); during actual measurements the AFL directly contacts the cell surface; (*Right*) epifluorescence of the same image indicating membrane expression of rprestin-GFP. (*B*) Amplitude and (*C*) phase of the mechanical force exerted on the AFL as a result of the electromechanical action of rprestin. Data points are from three individual experiments on CHO (■ and ●) or HEK293 cells (▲) transfected with rprestin-C_{GFP}; results from a mock-transfected CHO cell are given as control (○). Note that amplitude and phase are almost constant over the measured frequency range. (*D*) Effect of salicylate added to the bath on the rprestin-mediated force generation. Data points are for phase before (○), during (■), and after (●) addition of 10 mM salicylate to the bath; amplitudes were reduced by a factor of ≈2.5 over the entire frequency range (data not shown). The signal-to-noise ratio above 1 kHz was 18 dB before application and 10 dB in the presence of salicylate.

measurement, to determine the mechanical impedance, Z_{AFL} (32). The velocity of the AFL, V_{AFL}, in response to the electrical stimulation of the cell was measured with a laser Doppler vibrometer (Polytec 302, Waldbronn, Germany) focused on the AFL. The force exerted by the cell on the AFL was calculated as $V_{AFL} \cdot Z_{AFL}$. This is an underestimate of the force produced by the cell because the mechanical impedances of the cell, Z_C, and AFL were similar. The former was determined by vibrating the microchamber with known velocity, V_{CAP}, measuring the resulting V_{AFL} with the laser Doppler vibrometer and calculating $Z_C = Z_{AFL} \cdot V_{AFL}/(V_{CAP} - V_{AFL})$. This impedance measurement was made for a limited number of cells; the mean spring constant was 0.032 ± 0.016 N/m ($n = 4$). In other words, the electromechanical force produced by the cell was, on average, about twice that exerted on the AFL. Force data were not corrected for this factor. Forces below 1 pN could be detected with an averaging time of 8 s. Electrical stimuli were applied to an Ag/AgCl electrode in the microchamber with the reference electrode in the bath chamber. Stimuli were composed of a multitone complex of 58 sinusoids (9.1 spectral points per octave) of equal amplitude and random phase. All data shown are for a voltage amplitude of 10 mV per sinusoid. The electrical resistance of the microchamber for low frequencies (< 500 Hz) was, on average, 0.39 ± 0.04 MΩ ($n = 6$) without cell and 3.54 ± 1.87 MΩ ($n = 16$) with cell.

Results

Cloning rprestin. The rprestin full-length coding sequence as obtained with PCR-based techniques from a rat cochlea-specific cDNA library consists of 2,232 nt, encoding a polypeptide of 744 residues (Fig. 1*A*). Comparison with gerbil prestin (gprestin) indicated that the derived amino acid sequence of rprestin is 96.4% identical with gprestin, differences in sequence only occur in the distal N and C termini. When analyzed for hydrophobicity with the Kyte and Doolittle algorithm, rprestin presents with an overall hydrophobic core region that is flanked by mostly hydrophilic N and C termini (Fig. 1*B*).

To test for its subcellular distribution and localization of the hydrophilic N and C termini, rprestin was fused to the GFP and tagged with the HA tag (N_{HA}-rprestin-C_{GFP}). As shown by confocal fluorescence microscopy for expression in OK cells (Fig. 1*C*), rprestin was localized predominantly to the plasma membrane as recently reported (20, 33). Moreover, the N-terminal HA tag as well as the C-terminally fused GFP were accessible to the respective antibody only after permeabilization of the cells, whereas no staining was observed in nonpermeabilized cells (Fig. 1*C*). These findings localize N and C termini of rprestin to the cytoplasmic side of the membrane.

Electromechanical Properties of rprestin. Functionality of heterologously expressed rprestin was assessed with two methods: (*i*) by examining the expected voltage-dependent charge movement and (*ii*) by examining the ability to generate electromechanical force.

Charge movement was probed with the phase-tracking technique, a highly sensitive lock-in technique for direct measurement of membrane capacitance (34, 35). As shown in Fig. 2*A*, rprestin-expressing cells exhibited a bell-shaped C_{nonlin} in response to the transmembrane voltage ramped from −120 to 70 mV. This C_{nonlin}, which was observed in all cells injected with the rprestin-C_{GFP} fusion construct, was well fitted with the derivative

of a first-order Boltzmann function that describes the C_{nonlin} observed in OHCs (Eq. **1;** ref. 11). For rprestin-C_{GFP}, such fits yielded values for $V_{1/2}$, α, and Q_{max} of -75.5 ± 9.1 mV, 35.5 ± 2.3 mV, and 81.4 ± 44.8 fC, respectively ($n = 16$). These values were not affected by the fused GFP (values for rprestin were -69.7 ± 19.7 mV, 34.9 ± 5.5 mV, and 67.2 ± 51.3 fC for $V_{1/2}$, α, and Q_{max}, respectively; $n = 6$); $V_{1/2}$ and α were independent of whether C_{nonlin} was recorded in excised outside-out patches or in whole-cell patch-clamp configuration (Fig. 2*A Inset*; values for rprestin-C_{GFP} in outside-out patches were -71.9 ± 30.1 mV, 32.0 ± 4.8 mV, and 0.8 ± 1.3 fC for $V_{1/2}$, α, and Q_{max}, respectively ($n = 19$)). Equivalent data where obtained from transfected OK and HEK 293 cells. Moreover, Q_{max}, α, and $V_{1/2}$ were independent of the stimulus frequency used for phase tracking (1–5 kHz; data not shown). Fig. 2 *B* and *C* illustrates close agreement between the values characterizing C_{nonlin} mediated by rprestin in CHO cells and those obtained for the motor protein-mediated C_{nonlin} in rat OHCs. Moreover, slope (α) and $V_{1/2}$ of rprestin-mediated C_{nonlin} were not affected by coexpression of the fructose transporter GLUT5 that was suggested to be part of the motor protein complex (refs. 36 and 37; Fig. 2*C*).

Together, these results show that rprestin-mediated C_{nonlin} is virtually identical with the C_{nonlin} mediated by adult OHCs, although the maximum charge and charge density were lower in injected cells by roughly a factor of 10.

For the purpose of examining the ability of rprestin to produce electromechanical force, transfected cells were sucked into a microchamber and mechanical force was determined with an AFL placed onto the protruding end of the cell (Fig. 3*A*). In this configuration, rprestin resulted in forces of up to 3 pN upon stimulation with voltage sinusoids of 10 mV in the frequency range of 0.2 to 20 kHz (see *Materials and Methods*). Fig. 3 shows representative results from experiments with transfected CHO and HEK 293 cells. The amplitude of the rprestin-mediated force was largely constant over the entire frequency range (Fig. 3*B*). Similarly, the phase of the mechanical force relative to the electrical stimulus was constant over the whole frequency range and exhibited values roughly around $-180°$ (Fig. 3*C*). This means that, like the OHC motor, rprestin generates a contractile force upon depolarization of the membrane (5). Interestingly, mock-transfected cells also caused displacement of the AFL, probably due to movement of charged structures in the electrical field. However, the force derived for these cells was always lower in amplitude and the phase was 0° (control in Fig. 3 *B* and *C*).

To further test the specificity of the rprestin-mediated force response, its sensitivity to salicylate, known to reduce OHC motility (11, 38), was probed. As shown in Fig. 3*D*, the phase was reversibly shifted toward 0° by 10 mM salicylate applied to the bath medium; the amplitude was reduced by a factor of ≈ 2.5 on the entire frequency range (data not shown). Salicylate did not affect phase or amplitude of the motility in mock-transfected cells (data not shown).

These results indicate that rprestin expressed in culture cells is able to generate mechanical force upon electrical stimulation with characteristics very similar to those observed for the OHC motor protein.

Mechanoelectrical Properties of rprestin. rprestin was probed for reciprocal electromechanical properties known for the OHC motor protein (13–15) by examining the effect of membrane tension on the nonlinear charge movement. This was done by measuring C_{nonlin} in excised outside-out patches while varying membrane tension by application of a pressure of 40 hPa through the recording pipette. As shown in Fig. 4, pressure application reversibly shifted C_{nonlin} along the voltage axis toward more depolarized potentials. Thus, the voltage required for half-maximal charge movement ($V_{1/2}$) was changed by the increase in membrane tension by 20.6 ± 9.4 mV ($n = 6$). In contrast, the

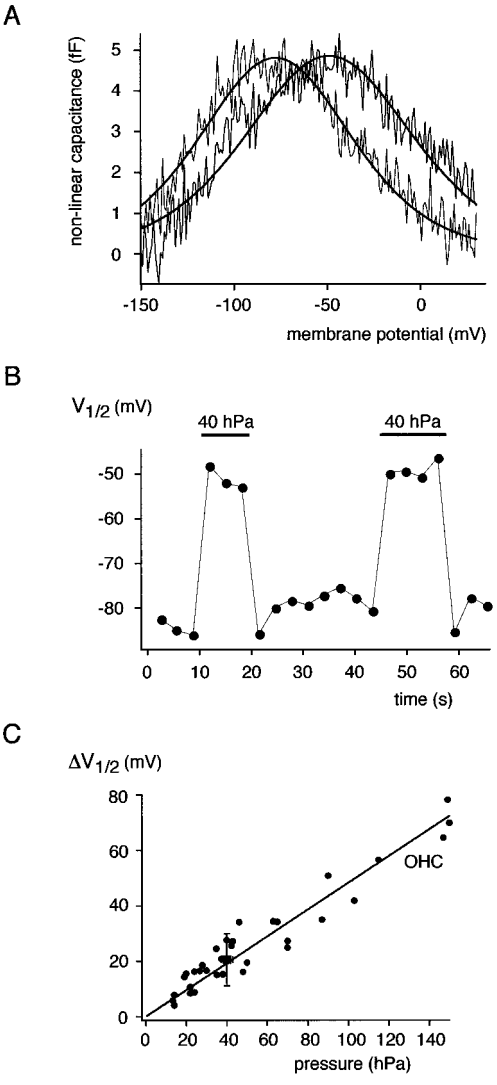

Fig. 4. Shift of the rprestin C_{nonlin} in response to mechanical stimulation. (*A*) C_{nonlin} measured in an excised outside-out patch before (gray trace) and during (black trace) application of 40 hPa to the back of the recording pipette. (*B*) $V_{1/2}$ values of C_{nonlin} determined from ramped phase-track recordings plotted as a function of time; application of 40 hPa is indicated by horizontal bars. Note the reversible shift in $V_{1/2}$ induced by the increase in membrane tension. (*C*) Pressure-induced shift in $V_{1/2}$ ($\Delta V_{1/2}$) of rprestin C_{nonlin} is identical to the $\Delta V_{1/2}$ obtained from OHCs. $\Delta V_{1/2}$ for rprestin is given as mean ± SD from five experiments with 40-hPa pressure application to outside-out patches (■; given as mean pressure ± SD, see *Materials and Methods*); the $\Delta V_{1/2}$ values obtained from outside-out patches of five OHCs at various pressure applications are given as individual data points (●). Line is fit of a regression line through the origin to the OHC data; slope of the line is 0.48 mV/hPa.

slope factor (α) characterizing the voltage dependence of C_{nonlin} remained essentially unchanged (Fig. 4*A*). These results on pressure-induced shift in $V_{1/2}$ are in close agreement with the respective pressure-$\Delta V_{1/2}$ relation obtained in patches excised from adult rat OHCs (Fig. 4*C*). Under identical conditions, the $V_{1/2}$ value of OHC C_{nonlin} increased upon pressure application with a slope of 0.48 mV/hPa (line in Fig. 4*C*). These results indicate that translocation of the rprestin voltage sensor is directly coupled to the mechanical tension of the plasma membrane.

Discussion

The results presented here demonstrate that rprestin is able to act as a molecular motor that reproduces the quasi-

piezoelectrical properties conceptually assigned to the motor protein of OHCs (7, 18). Thus, rprestin generates force upon electrical stimulation at stimulus frequencies of up to at least 20 kHz (Fig. 3), and translocation of its charged voltage sensor occurring in the same frequency range is coupled to the mechanical properties of the plasma membrane (Fig. 4).

In particular, the results strongly support the concept of a single protein working as an electromechanical transducer, as suggested by Zheng *et al.* (20). Accordingly, our experiments show that reciprocal electromechanical properties of rprestin did not require the particular environment provided by OHCs, including the highly specialized cytoskeleton (21). These components are supposed to be missing or to be at least different in the culture cells used for heterologous expression of rprestin (including CHO, HEK293, and OK cells). Moreover, cytoskeletal elements certainly disturbed in excised patches were not required for mechanical coupling of C_{nonlin} to membrane tension (Fig. 4). It should be added, however, that cytoskeleton and/or cell shape seemed to be important in our experiments for effective conversion of molecular events to the force detected by the AFL; thus, the amplitude of the rprestin-generated force was impaired when cells were protease-treated for detachment from their support before experiments as in Fig. 3.

Moreover, there is no indication that functional rprestin might require further molecular components or additional subunits, given that all characteristics of the molecule faithfully reproduce the properties of the OHC motor. Coexpression of GLUT5, a fructose transporter recently suggested to participate in a putative motor protein complex (37), did not affect the electrical properties of rprestin as indicated by the unchanged C_{nonlin} (Fig. 2*C*).

Although rprestin is very likely to represent the force-generating motor of OHCs, the actual molecular process(es) that "work the work" remain largely unknown. Namely, the voltage sensor of the protein, as well as the domains undergoing structural rearrangements that change the molecule's area in the membrane, await identification. Furthermore, the variation in the $V_{1/2}$ value of C_{nonlin} observed in patches excised from rprestin-expressing cells (Fig. 2*B*) is likely to correspond to a regulation phenomenon observed during hair cell development (Fig. 2*B*; ref. 28) and in adult OHCs (39). The underlying mechanisms remain to be addressed at the molecular level.

We thank Drs. U. Schulte and J. P. Ruppersberg for helpful discussions; S. Eble, S. Weidemann, and J. Wöltjen for excellent technical assistance; and Dr. M. Kasahara for kindly providing the GLUT5 cDNA. This work was supported by the Deutsche Forschungsgemeinschaft (Grant SFB 430/A1 to B.F.) and the Interdisziplinäres Zentrum für klinische Forschung Tübingen (01KS9602, project IA2 to A.W.G.).

1. Ashmore, J. F. (1987) *J. Physiol. (London)* **388,** 323–347.
2. Brownell, W. E., Bader, C. R., Bertrand, D. & de Ribaupierre, Y. (1985) *Science* **227,** 194–196.
3. Kachar, B., Brownell, W. E., Altschuler, R. & Fex, J. (1986) *Nature (London)* **322,** 365–368.
4. Dallos, P. & Evans, B. N. (1995) *Science* **267,** 2006–2009.
5. Frank, G., Hemmert, W. & Gummer, A. W. (1999) *Proc. Natl. Acad. Sci. USA* **96,** 4420–4425.
6. Russell, I. J. & Nilsen, K. E. (1997) *Proc. Natl. Acad. Sci. USA* **94,** 2660–2664.
7. Dallos, P., Evans, B. N. & Hallworth, R. (1991) *Nature (London)* **350,** 155–157.
8. Holley, M. C. & Ashmore, J. F. (1988) *Proc. R. Soc. London Ser. B* **232,** 413–429.
9. Gale, J. E. & Ashmore, J. F. (1997) *Nature (London)* **389,** 63–66.
10. Ashmore, J. F. (1989) in *Mechanics of Hearing*, eds. Wilson, J. P. & Kemp, D. (Plenum, New York), Vol. A164**,** pp. 107–113.
11. Santos-Sacchi, J. (1991) *J. Neurosci.* **11,** 3096–3311.
12. Tunstall, M. J., Gale, J. E. & Ashmore, J. F. (1995) *J. Physiol. (London)* **485,** 739–752.
13. Gale, J. E. & Ashmore, J. F. (1994) *Proc. R. Soc. London Ser. B* **255,** 243–249.
14. Iwasa, K. H. (1993) *Biophys. J.* **65,** 492–498.
15. Kakehata, S. & Santos-Sacchi, J. (1995) *Biophys. J.* **68,** 2190–2197.
16. Kalinec, F., Holley, M. C., Iwasa, K. H., Lim, D. J. & Kachar, B. (1992) *Proc. Natl. Acad. Sci. USA* **89,** 8671–8675.
17. Dallos, P., Hallworth, R. & Evans, B. N. (1993) *J. Neurophysiol.* **70,** 299–323.
18. Iwasa, K. H. (1994) *J. Acoust. Soc. Am.* **96,** 2216–2224.
19. Forge, A., Davies, S. & Zajic, G. (1991) *J. Neurocytol.* **20,** 471–484.
20. Zheng, J., Shen, W., He, D. Z., Long, K. B., Madison, L. D. & Dallos, P. (2000) *Nature (London)* **405,** 149–155.
21. Holley, M. C., Kalinec, F. & Kachar, B. (1992) *J. Cell Sci.* **102,** 569–580.
22. Frohman, M. A. (1993) *Methods Enzymol.* **218,** 340–356.
23. Zhang, Y. & Frohman, M. A. (1997) *Methods Mol. Biol.* **69,** 61–87.
24. Ho, S. N., Hunt, H. D., Horton, R. M., Pullen, J. K. & Pease, L. R. (1989) *Gene* **77,** 51–59.
25. Kozak, M. (1986) *Cell* **44,** 283–292.
26. Kozak, M. (1987) *Nucleic Acids Res.* **15,** 8125–8148.
27. Klöcker, N., Oliver, D., Ruppersberg, J. P., Knauss, H. G. & Fakler, B. (2000) *Mol. Cell. Neurosci.*, in press.
28. Oliver, D., Klocker, N., Schuck, J., Baukrowitz, T., Ruppersberg, J. P. & Fakler, B. (2000) *Neuron* **26,** 595–601.
29. Herrington, J. D., Newton, K. R. & Bookman, R. J. (1995) *Pulse Control V4.4: IGOR XOPs for Patch-Clamp Data Acquisition and Capacitance Measurements* (Univ. of Miami, Miami, FL).
30. Oliver, D. & Fakler, B. (1999) *J. Physiol. (London)* **519,** 791–800.
31. Evans, B. N., Dallos, P. & Hallworth, R. (1989) in *Cochlear Mechanics*, eds. Wislon, J. P. & Kemp, D. T. (Plenum, New York), pp. 205–206.
32. Scherer, M. P., Frank, G. & Gummer, A. W. (1999) *J. Appl. Phys.* **88,** 2912–2920.
33. Belyantseva, I. A., Adler, H. J., Curi, R., Frolenkov, G. I. & Kachar, B. (2000) *J. Neurosci.* **20,** RC116, 1–5.
34. Fidler, N. & Fernandez, J. M. (1989) *Biophys. J.* **56,** 1153–1162.
35. Neher, E. & Marty, A. (1982) *Proc. Natl. Acad. Sci. USA* **79,** 6712–6716.
36. Ashmore, J. F., Geleoc, G. S. & Harbott, L. (2000) *Proc. Natl. Acad. Sci. USA* **97,** 11759–11764.
37. Geleoc, G. S., Casalotti, S. O., Forge, A. & Ashmore, J. F. (1999) *Nat. Neurosci.* **2,** 713–719.
38. Russell, I. J. & Schauz, C. (1995) *Aud. Neurosci.* **1,** 309–319.
39. Frolenkov, G. I., Mammano, F., Belyantseva, I. A., Coling, D. & Kachar, B. (2000) *J. Neurosci.* **20,** 5940–5948.